Maternal expression of the checkpoint protein BubR1 is required for synchrony of syncytial nuclear divisions and polar body arrest in *Drosophila melanogaster*

Daniel Pérez-Mongiovi[1,*], Nicolas Malmanche[1,*], Hassan Bousbaa[1,2] and Claudio Sunkel[1,3,†]

[1]Instituto de Biologia Molecular e Celular, Universidade do Porto, Rua do Campo Alegre 823, 4150-180 Porto, Portugal
[2]Instituto Superior de Ciências da Saúde-Norte, Grupo de Biologia Molecular e Celular, Rua Central de Gandra 1317, 4580 Gandra PRD, Portugal
[3]ICBAS, Instituto de Ciências Biomédicas de Abel Salazar, Universidade do Porto, 4000 Porto, Portugal
*These authors contributed equally to this work
†Author for correspondence (e-mail: cesunkel@ibmc.up.pt)

Accepted 5 August 2005

Development 132, 4509-4520
Published by The Company of Biologists 2005
doi:10.1242/dev.02028

Summary

The spindle checkpoint is a surveillance mechanism that regulates the metaphase-anaphase transition during somatic cell division through inhibition of the APC/C ensuring proper chromosome segregation. We show that the conserved spindle checkpoint protein BubR1 is required during early embryonic development. BubR1 is maternally provided and localises to kinetochores from prophase to metaphase during syncytial divisions similarly to somatic cells. To determine BubR1 function during embryogenesis, we generated a new hypomorphic semi-viable female sterile allele. Mutant females lay eggs containing undetectable levels of BubR1 show early developmental arrest, abnormal syncytial nuclear divisions, defects in chromosome congression, premature sister chromatids separation, irregular chromosome distribution and asynchronous divisions. Nuclei in BubR1 mutant embryos do not arrest in response to spindle damage suggesting that BubR1 performs a checkpoint function during syncytial divisions. Furthermore, we find that in wild-type embryos BubR1 localises to the kinetochores of condensed polar body chromosomes. This localisation is functional because in mutant embryos, polar body chromatin undergoes cycles of condensation-decondensation with additional rounds of DNA replication. Our results suggest that BubR1 is required for normal synchrony and progression of syncytial nuclei through mitosis and to maintain the mitotic arrest of the polar body chromosomes after completion of meiosis.

Key words: BubR1, Mitosis, Checkpoint, Embryogenesis, Polar body, *Drosophila*

Introduction

The first stages of *Drosophila* embryonic development occur within a syncytium into which 10 synchronous and three meta-synchronous nuclear divisions take place. These events are under the control of maternally provided protein and mRNA before cellularisation (Edgar et al., 1994; Foe et al., 1993). During each of the first 10 syncytial cycles, nuclei alternate between S and M phases without intervening gap phases. Until cycle 8, Cdk1 activity and cyclin B levels do not oscillate and the cycles are driven autonomously by the mitotic apparatus rather than by mitotic regulators (Edgar et al., 1994). Subsequently, the cycles gradually slowdown becoming meta-synchronous and from cycles 8 to 13 depend upon cyclin B activity. It has been suggested that the delays induced by cell cycle checkpoints would not be compatible with the rapid and synchronous syncytial divisions and damaged nuclei are though to be eliminated by a mechanism that aims to preserve normal early development (Edgar et al., 1994; Foe et al., 1993).

Current studies of the mitotic checkpoint proteins Mad2 and Bub3 indicate that spindle checkpoint activity is required for proper chromosome segregation within the epiblast of the mouse embryo at the time of rapid nuclear proliferation (Dobles et al., 2000; Kalitsis et al., 2000). In the *Drosophila* syncytial embryo, global perturbations such as blocking DNA replication, inducing extensive DNA damaged, or blocking spindle assembly are known to arrest or delay mitosis throughout the syncytium (Callaini et al., 1994; Debec et al., 1996; Fogarty et al., 1997; Raff and Glover, 1988). Interestingly, embryonic expression of a non-degradable form of cyclin B or increase maternal cyclin B contribution can affect the global behaviour of nuclear cycles (Ji et al., 2002; Su et al., 1998). In addition, syncytial mutant embryos for the mitotic checkpoint protein Mps1 fail to arrest in mitosis in response to hypoxia (Fischer et al., 2004). It has been recently proposed that embryogenesis between mammals and other metazoans such as fly or frog should be aligned not from fertilisation but from the rapid embryonic cell cycles (O'Farrell et al., 2004). Thus, mammalian peri-gastrulation cell cycles should be homologous to the rapid cleavages cycles of other metazoans, such as syncytial cycles in flies. Therefore, mitotic checkpoint proteins could have an important and conserved

role in monitoring rapid embryonic cell divisions in different and evolutionary distant metazoans.

Mitotic checkpoint proteins detect microtubule attachment and/or tension applied across kinetochore pairs to ensure that chromatids separate during mitosis only when kinetochores form stable bipolar microtubule attachments (Musacchio and Hardwick, 2002). Current studies indicate that the well-conserved Bub and Mad proteins play an essential role in the spindle checkpoint function. These proteins inhibit the activity of the anaphase promoting complex or cyclosome (APC/C) until microtubule attachment/tension is achieved for all chromosomes (Peters, 2002; Zachariae and Nasmyth, 1999). BubR1 is an essential spindle checkpoint protein conserved among higher eukaryotic organisms (Chan et al., 1998; Chen, 2002). Recently, it has been shown that the previously identified Bub1 protein in *Drosophila* (Basu et al., 1999) should be reclassified as BubR1 (Logarinho et al., 2004). In *Drosophila* somatic cells, BubR1 loss of function mutation causes an accelerated transit through mitosis which leads to abnormal chromosome segregation and apoptosis (Basu et al., 1999).

In order to analyse whether BubR1 is required during the nuclear proliferation at the syncytial stages in *Drosophila* embryos, we characterised a new semi-viable female sterile hypomorphic allele (*bubR1*^{Rev1}) that was produced by imprecise excision of a previously characterised P element insertion (Basu et al., 1999). In embryos from homozygous *bubR1*^{Rev1} mutant females, syncytial nuclei show defects similar to those observed in neuroblasts homozygous for the *bubR1*^{1} allele and do not arrest in mitosis in response to microtubule depolymerisation. In addition, whereas in wild-type embryos the 10 first syncytial nuclear divisions are synchronous, embryos from homozygous *bubR1*^{Rev1} mutant females show severe nuclear de-synchronisation. Furthermore, BubR1 accumulates at the kinetochores of the highly condensed polar body chromosomes. Analysis of fertilised embryos from homozygous *bubR1*^{Rev1} mutant females indicates that BubR1 is required to maintain the condensed conformation of polar body chromosomes and to exclude it from the mitotic oscillation.

Materials and methods

Drosophila stocks

bubR1^{Rev1} was obtained by imprecise excision of the P-element in *1(2)K03113* (Basu et al., 1999; Cooley et al., 1988). Histone-GFP transgene 62A was used for live imaging of syncytial nuclei and polar body (Clarkson and Saint, 1999). Fertilised mutant embryos were obtained by crossing homozygous *bubR1*^{Rev1} females with wild-type males (w^{1118}).

Southern blotting

Genomic DNA was extracted according to Roberts (Roberts, 1986) from adult flies frozen in liquid nitrogen and digested with *Hin*dIII and *Eco*RI (New England Biolabs). Southern blots were done according to Sambrook et al. (Sambrook et al., 1989) and probed with a complete cDNA (see Fig. 2A).

Western blotting

Third larval instar brains, adult female ovaries and embryos were dissected in 1×PBS, transferred to sample buffer [50 mM Tris (pH 6.8), 100 mM DTT, 2% SDS, 0,1% Bromophenol Blue and 10% glycerol] heated 3 minutes at 95°C before SDS-page (7.5%) migration. Proteins were transferred onto Immobilon-P membrane (Schleicher & Schuell) and probed with anti-DmBubR1 rabbit polyclonal antibodies (Rb666 Ab) (Logarinho et al., 2004), diluted 1:2500 in PBST (1× PBS and 0.2% Triton-100) containing 1% BSA (Sigma) and 2% dried non-fat milk. Anti-α-tubulin was detected using mouse mAb B512 (Sigma-Aldrich), diluted 1:2000. Secondary antibodies conjugated to HRP (Vector, UK) were used according to the manufacturer's instructions. Detection of antibody signals was performed with the ECL system (Amersham).

Immunofluorescence of embryos

Embryos were collected and aged at 25°C and processed as previously (Sullivan et al., 2000). Primary antibodies were: anti-BubR1 (Rb666) antibody pre-adsorbed on wild-type 0-2 hours embryos at a 1:10 dilution and used at 1:1000 dilution; anti-α-tubulin (mouse mAb B512), used at 1:3000 (Sigma-Aldrich); anti-phospho H3 rabbit polyclonal, used at 1:500 (Upstate Biotechnology); anti-CID chicken polyclonal, used at 1:1000 (Blower and Karpen, 2001); anti-CNN rabbit polyclonal, used at 1:1000 (Heuer et al., 1995); anti-BrdU mouse monoclonal primary antibody, used at 1:50 (Sigma-Aldrich). Secondary antibodies were: anti-rabbit Alexa Fluor 488 used at 1:2000 (Molecular Probes), anti-mouse Alexa Fluor 568 used at 1:2000 (Molecular Probes) or anti-chicken Cy5 used at 1:200 (Jackson). Samples were mounted in Vectashield (Vector, UK) containing 1 μg/ml of DAPI or 1.0 μg/ml propidium iodide. Observation and images were obtained using Zeiss Axiovert 200M microscope (Zeiss, Germany) or a Leica TCS SP2 AOBS Confocal Microscope (Leica Microsystems, Heidelberg). Images were deconvolved and processed with Adobe Photoshop 7.0. For colchicine treatment, embryos were permeabilised in n-heptane, containing 250 μM colchicine in 1× PBS for 30 minutes before fixation. For BrdU incorporation, the embryos were permeabilised for 4 minutes in n-octane followed by 8-10 minutes BrdU pulse at 1 mg/ml in 1× PBS before fixation.

Live imaging

Chromosomes in wild-type and *bubR1*^{Rev1} embryos were visualised by time-lapse recording of the Histone-GFP transgene. Images were taken every 10 or 15 seconds using a BioRad MRC600 Confocal Microscopy with two scans per image. To determine the polar body Histone-GFP signal intensity over time, we repeated three measurements of a restricted area of 16 pixels taken from regions with higher intensity signal and use ImageJ software to obtain an average and standard deviation for each image. Using the same measurements, we calculated the average standard deviation pixel intensity of the recorded period of time.

Results

Immunolocalisation of BubR1 during embryogenesis

BubR1 localisation has been described in somatic cells of different organisms, including *Drosophila* (Basu et al., 1999), but it has never been characterised during the syncytial stages of *Drosophila* embryos. Accordingly, we analysed the localisation of BubR1 at 0-180 minutes after egg laying (AEL) in wild-type embryos (Fig. 1). BubR1 was first detected at kinetochores of mitotic chromosomes during prophase and became stronger in prometaphase. During metaphase, BubR1 kinetochore staining decrease significantly and during anaphase it was undetectable (Fig. 1A-J). BubR1 localisation follows the same pattern during early (Fig. 1A-E) or late (Fig. 1F-J) cycles. Co-localisation with anti-CID antibody shows that BubR1 accumulates at kinetochores of condensed

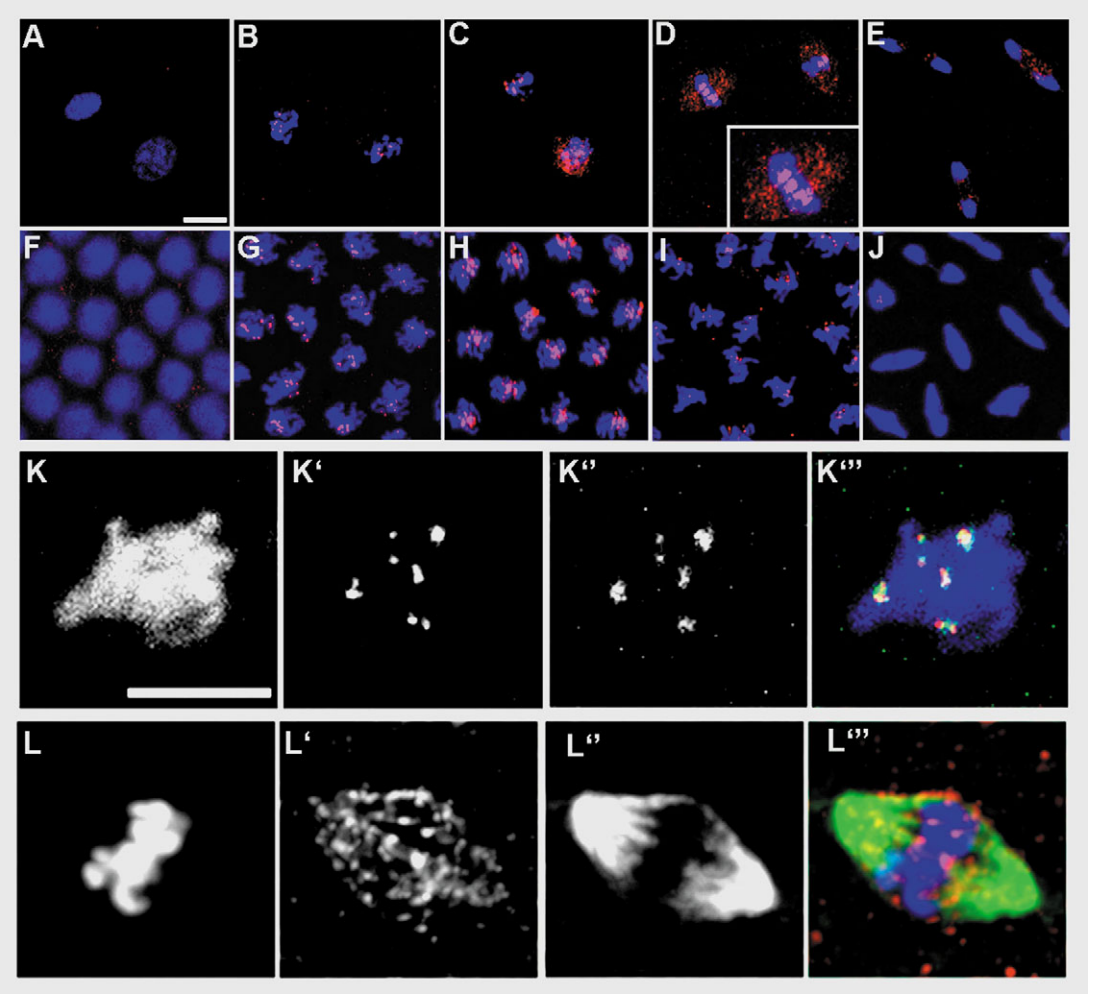

Fig. 1. Immunolocalisation of BubR1 during syncytial divisions. In all images, DNA is stained blue and BubR1 is stained red. (A-E) BubR1 immunolocalisation during syncytial nuclear division cycles 3-9 and (F-J) cycles 10-13. (A,F) BubR1 shows no specific localisation during interphase but (B,G) starts to accumulate at the kinetochores in prophase, (C,H) reaching a maximum in prometaphase, (D,I) decreases at metaphase and (E,J) is absent at anaphase. (K,K′′′) High-magnification view of a syncytial nucleus in prophase showing co-localisation of BubR1 and CID (shown in green). (K) Chromosome morphology at prophase showing initiation of condensation. (K′) BubR1 co-localises with (K′′) CID at kinetochores of prophase chromosomes. (K′′′) Merged image showing colocalisation of BubR1 and CID. (L,L′′′) High-magnification view of a syncytial nucleus at metaphase showing co-localisation of BubR1 over spindle microtubules (green). (L) Chromosome morphology at metaphase showing alignment along the metaphase plate. (L′) At metaphase, BubR1 is sometimes detected along spindle microtubules (see also inset in D). (L′′) Spindle microtubules were detected with anti-α-tubulin antibodies. (L′′′) Merged image showing co-localisation of BubR1 along spindle microtubules. Scale bar: 10 μm.

chromosomes (Fig. 1K-K′′′). In addition, we detected BubR1 on spindle microtubules at metaphase (inset in Fig. 1D and Fig. 1L,L′′′). Overall, our results indicate that BubR1 protein has a dynamic pattern of kinetochore localisation, consistent with its role in monitoring microtubule kinetochore interaction during the syncytial nuclear cycles of *Drosophila* embryos.

Molecular and phenotypic characterisation of a hypomorphic *bubR1* allele

To study the role of BubR1 in embryogenesis, we characterised a new hypomorphic semi-viable female sterile *bubR1* allele (*bubR1*^{Rev1}) obtained by imprecise excision of the lethal P element in *bubR*^{1} (Basu et al., 1999; Cooley et al., 1988). *bubR1*^{Rev1} was found to be semi-lethal and ~10% of the homozygous reach adult stages. Homozygous mutant females are sterile and lay fewer eggs than wild-type flies. Molecular analysis indicated that the P element present in *bubR1*^{Rev1} has an internal deletion of ~2 kb (Fig. 2A,B). PCR with a combination of appropriate primers of the ends of the P-element confirm this conclusion (Fig. 2A and data not shown). In the course of the reversion screen, we also identified a perfect excision allele (rev74) for which southern blot, homozygous viability and fertility were indistinguishable from the wild-type control (Fig. 2A,B and data not shown), indicating that the semi-lethality of *bubR1*^{Rev1} homozygote adults and the lethality and phenotype of embryos derived from *bubR1*^{Rev1}/*bubR1*^{Rev1} females results from the P element present in this line.

BubR1 protein levels in wild-type and mutant alleles at various developmental times were determined by western blotting (Fig. 2C). High levels of BubR1 were detected in wild-type third instar larval brains and ovaries. In *bubR1*^{1}/*bubR1*^{1}

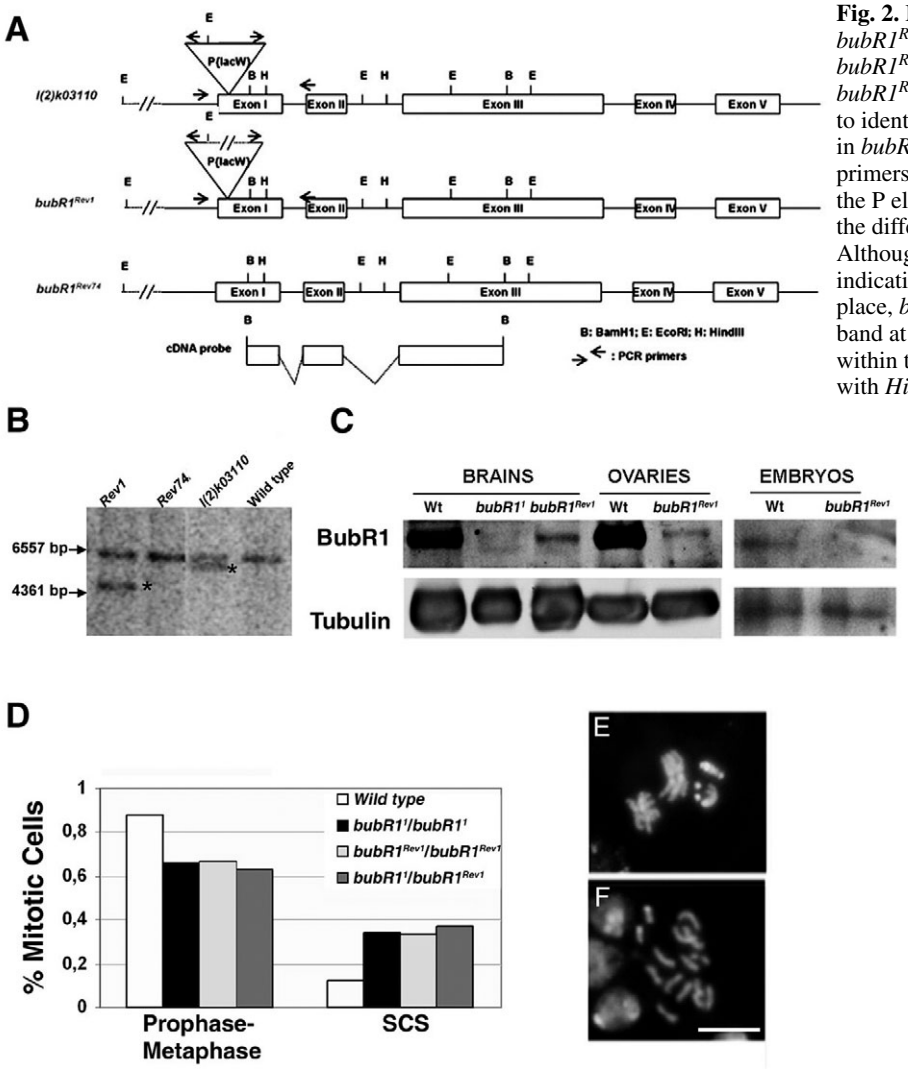

Fig. 2. Molecular and phenotypic characterisation of *bubR1*^{Rev1}. (A) Genomic organisation of *bubR1*^{1}, *bubR1*^{Rev1} and *bubR1*^{Rev74} alleles. *bubR1*^{Rev1} and *bubR1*^{Rev74} were isolated from a genetic screen designed to identify imprecise excisions of the P element inserted in *bubR1*^{1} (*l(2)K03110*). Arrows indicate pairs of primers used for PCR to determine whether the ends of the P elements were intact. (B) Southern blot showing the difference between wild-type and *bubR1* alleles. Although *bubR1*^{Rev74} and wild-type strains are identical, indicating that a perfect P element excision had taken place, *bubR1*^{Rev1} genomic organisation shows a smaller band at 4.3 kb (asterisk), indicating a 2 kb deletion within the P element. The genomic DNA was digested with *Hin*dIII and *Eco*RI. (C) Western blot analysis of BubR1 protein levels in wild-type and *bubR1* alleles. Tubulin was used as a loading control. Total proteins from wild-type third instar larval brains and female ovaries shows high levels of BubR1. BubR1 could only be detected from a minimum of two wild-type embryo extract at 30-90 minutes AEL. Homozygous *bubR1*^{1} and *bubR1*^{Rev1} third instar larval brains show a significant reduction in BubR1 protein levels. BubR1 protein level is significantly decreased in homozygous *bubR1*^{Rev1} ovaries and undetectable from protein extract of two *bubR1*^{Rev1} embryos. (D) Quantification of the mitotic phenotype in third instar larval brains from wild-type and *bubR1* mutant allele combinations. In mutant genetic background, we observed a decrease in prometaphase-metaphase mitotic figures and an increase in the level of Sister Chromatid Separation (SCS). (E,F) Third instar larval neuroblasts incubated in 10 μM colchicine for 30 minutes induces a prometaphase-like arrest in wild-type cells (E), whereas most *bubR1*^{Rev1} mutant cells (F) undergo SCS. Scale bar: 5 μm.

brains, no protein is detected, while in *bubR1*^{Rev1}/*bubR1*^{Rev1} brains and ovaries there is a strong decrease in protein levels. BubR1 protein in ovaries results from somatic expression during the cell proliferation stages, the germline expression during cyst formation and the maternal contribution (data not shown). BubR1 could also be detected by western blot of embryo extracts at 30-90 minutes AEL using two wild-type embryos (Fig. 2C). However, in embryos derived from *bubR1*^{Rev1} homozygous females, the level of BubR1 was undetectable (Fig. 2C).

We also analyzed the mitotic behaviour and spindle checkpoint response of neuroblasts carrying different *bubR1* allelic combinations (Fig. 2D). *bubR1*^{1}/*bubR1*^{1}, *bubR1*^{1}/*bubR1*^{Rev1} and *bubR1*^{Rev1}/*bubR1*^{Rev1} mutant neuroblasts show a significant decrease in prophase-metaphase mitotic figures and a significant increase in sister chromatid separation (Fig. 2D). Furthermore, *bubR1*^{Rev1}/*bubR1*^{Rev1} neuroblasts fail to show a mitotic arrest in response to spindle damage (compare Fig. 2E with 2F). Accordingly, we suggest that *bubR1*^{Rev1} is a new hypomorphic allele and embryos derived from *bubR1*^{Rev1} homozygous females, fertilised by wild-type males, will, from now on, be designated as *bubR1*^{Rev1} embryos.

Analysis of nuclear divisions in *bubR1*^{Rev1} embryos

To determine whether BubR1 was required for nuclear divisions during early embryogenesis, we analysed *bubR1*^{Rev1} embryos (Fig. 3A-J). Quantitative analysis of fixed *bubR1*^{Rev1} embryos (n=80) at 120 to 150 minutes AEL showed that ~25% of the embryos stop development before cycle 10 (when nuclei reach the cortex); 62% developed up to cycle 10-13, although nuclei are not found evenly distributed throughout the cortex and they did not cellularise; 10% initiated cellularisation; and only 3% gastrulate but show pyknotic nuclei (Fig. 3H). *bubR1*^{Rev1} embryos accumulate defective nuclei throughout the syncytial stages and after cycle 10, most had many regions without cortical nuclei, extensive areas contained micronuclei, abnormally larger sized nuclei or paired nuclei with extensive DNA bridges (Fig. 3A-G). *bubR1*^{Rev1} embryos also showed abnormal mitotic progression, including precocious sister chromatid separation, lagging chromosomes, DNA bridges, irregular chromosome segregation and aneuploidy (Fig. 3E-G). A similar range of abnormalities was also observed in nuclei within mitotic domains of cellularised embryos (Fig. 3H).

To obtain a more accurate description of mitotic progression in *bubR1*^{Rev1} embryos, we quantified the relative frequency of

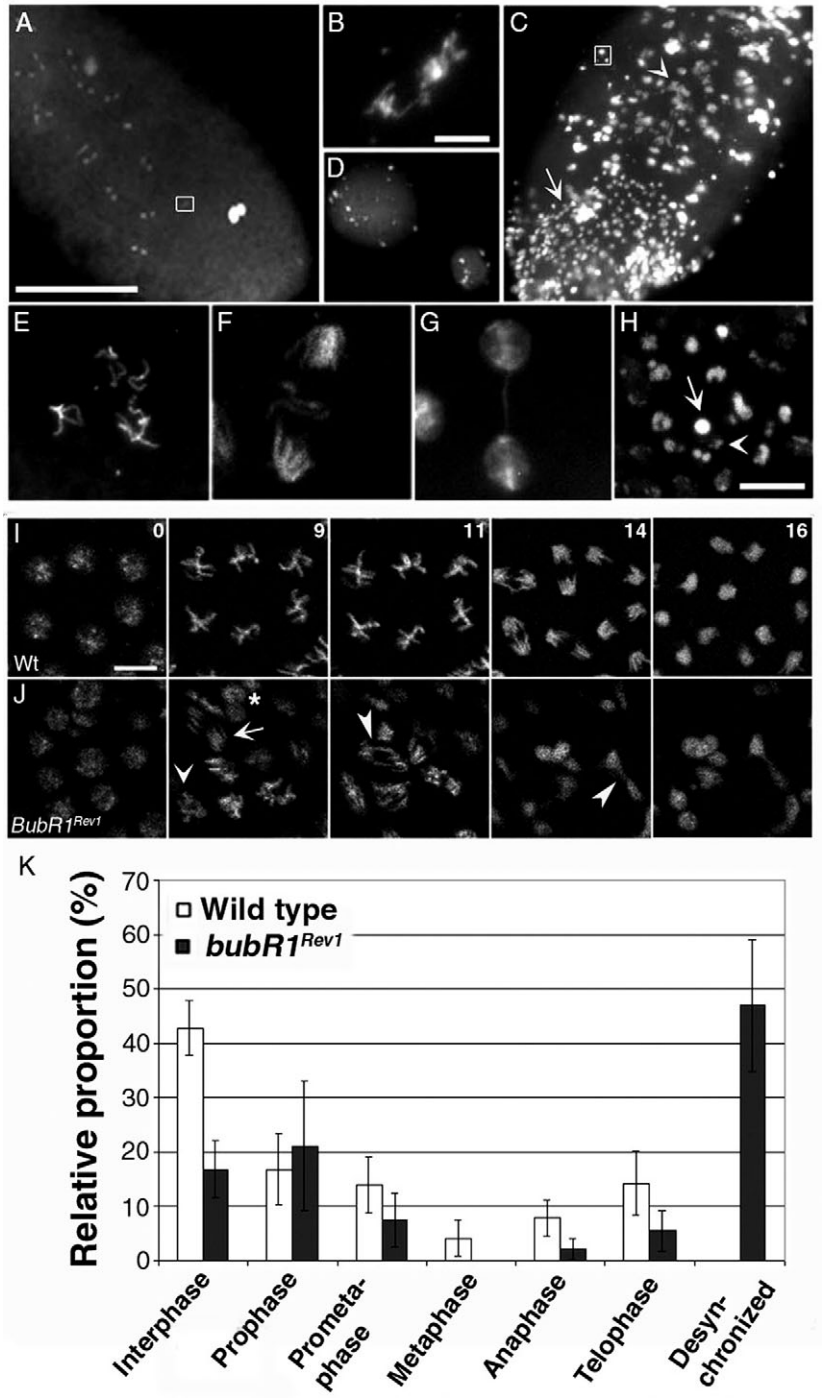

Fig. 3. Mitotic phenotypes in syncytial *bubR1*^{Rev1} embryos. (A) *bubR1*^{Rev1} embryos at nuclear cycle 5 in anaphase configuration. (B) Higher magnification view from a selected nuclei in A showing abnormal anaphase with asymmetric distribution of chromatin and lagging chromosomes. (C) *bubR1*^{Rev1} embryo at late syncytial stage showing irregular distribution and size of nuclei (see higher magnification in D) at the cortex (arrow) or at the interior of the embryo (arrowhead). (E-G) Abnormal mitotic progression in *bubR1*^{Rev1} embryos. (E) Prometaphase nuclei showing precocious sister chromatid separation, (F) anaphase nuclei showing lagging chromosomes and (G) telophase nuclei showing DNA bridges. (H) Mitotic domain of a gastrulated *bubR1*^{Rev1} embryo showing micronuclei (arrowhead) and pyknotic nuclei (arrow). Nuclei from wild-type (I) or *bubR1*^{Rev1} embryos (J) were imaged by time-lapse confocal microscopy of the Histone-GFP transgene during mitosis. Recording was performed from early stages of chromosome condensation until late telophase; the time is indicated in minutes in every frame (see Movies 1 and 2 in the supplementary material). Wild-type nuclei show normal chromosome congression and segregation. In *bubR1*^{Rev1} embryos, chromosomes never reach a stable metaphase configuration (arrowhead) and adjacent nuclei show highly asynchronous mitotic figures from prophase (asterisk) to anaphase (arrow). Aberrant chromosome segregation, such as lagging chromosomes (arrowhead at 11 minutes) and chromatin bridges (arrowhead at 14 minutes) are visible during anaphase and telophase. (K) Quantification of syncytial nuclear cycle stage in wild-type (n=259) and in *bubR1*^{Rev1} embryos (n=131) was performed on fixed material. Wild-type embryos show synchronous nuclei, while approximately half of the *bubR1*^{Rev1} embryos show desynchronised nuclear cycles. There is also a relative increase in prophase figures and we failed to detect any proper metaphases in *bubR1*^{Rev1} embryos. Scale bars: 100 μm in A,C; 25 μm in B,D-G; 50 μm in H; 10 μm in I,J.

mitotic figures in 30-90 minutes AEL embryos after fixation (Fig. 3K). We also visualised in vivo the behaviour of chromosomes using a GFP-Histone transgene (Clarkson and Saint, 1999) (Fig. 3I,J; see Movies 1 and 2 in the supplementary material). Quantification of the mitotic figures on fixed material reveals that, whereas in wild-type embryos all nuclei undergo synchronous division, almost half of the *bubR1*^{Rev1} embryos show asynchronous nuclear behaviour following cycle 5. Among the synchronous embryos, we observed a significant decrease in interphase nuclei and we never observed proper metaphase alignment. Live recording shows that the divisions in mutant embryos are highly asynchronous compared with the meta-synchronous divisions in wild-type controls (see Movies 1 and 2 in the supplementary material). In *bubR1*^{Rev1} embryos, nuclei in anaphase (Fig. 3J at 9 minutes), in prophase (Fig. 3J at 9 minutes) and nuclei initiating sister chromatid separation (Fig. 3J at 9 minutes) can be found at the same time. At later times, some nuclei show unequal chromosome segregation with lagging chromatids (Fig. 3J at 11 minutes) and chromatin bridges (Fig. 3J at 14 minutes). In addition, during mitotic progression, cytoplasmic movements are strongly affected in mutant embryos (compare Movie 1 with 2 in the supplementary material). Taken together these results indicate that BubR1 activity is required during

early embryonic development to maintain nuclear synchrony and cytoplasmic flux, and to prevent abnormal chromosome segregation.

Centrosome replication in *bubR1*^{Rev1} embryos

Coordination between local events of centrosome duplication, microtubule dynamics, changes in nuclear structure and positioning are essential for the correct spatial organisation of the early embryo. It has been recently proposed that regulation of DNA replication/segregation and centrosome function are coupled during the late syncytial divisions through a checkpoint mechanism designed to eliminate abnormal nuclei from the embryo (Fogarty et al., 1997; Sibon et al., 2000; Takada et al., 2003). However, an alternative model suggests that the *grape* gene coordinates nuclear envelope breakdown with chromosome condensation (Yu et al., 2000). In *bubR1*^{Rev1} embryos, in vivo analysis of the syncytial nuclear divisions show abnormal mitotic progression and cytoplasmic flux, suggesting that the coordination between these events was severely perturbed (see Movie 2 in the supplementary material). Cortical nuclei in the wild-type blastoderm embryos show a correlation between centrosomes pairs and nuclei (Fig. 4A). However, in *bubR1*^{Rev1} embryos, more than 90% of the embryos observed at a similar stage (cycles 10-13) showed cortical areas devoid of nuclei with abundant free centrosomes probably left at the cortex after nuclei had fallen into the embryo (Fig. 4C). In addition, during the syncytial stage many nuclei appear to loose their attachment to centrosomes as we observed centrosomes migration to the cortex in the absence of DNA (Fig. 4B).

As free centrosomes can be detected in *bubR1*^{Rev1} embryos, we analysed the relation between the nuclear cycle and the centrosome number over time. For this, we quantify centrosomes in individual *bubR1*^{Rev1} and wild-type embryos collected throughout the syncytial stages and plotted centrosome numbers by unit of space as a function of developmental time (Fig. 4D). Because at the time of cellularisation the centrosome number in *bubR1*^{Rev1} embryos is 30-40% higher relative to the control, our results indicate that centrosomes initiate an extra round of replication, which is never fully completed. We also found a small number of embryos (<5%) that had very few nuclei

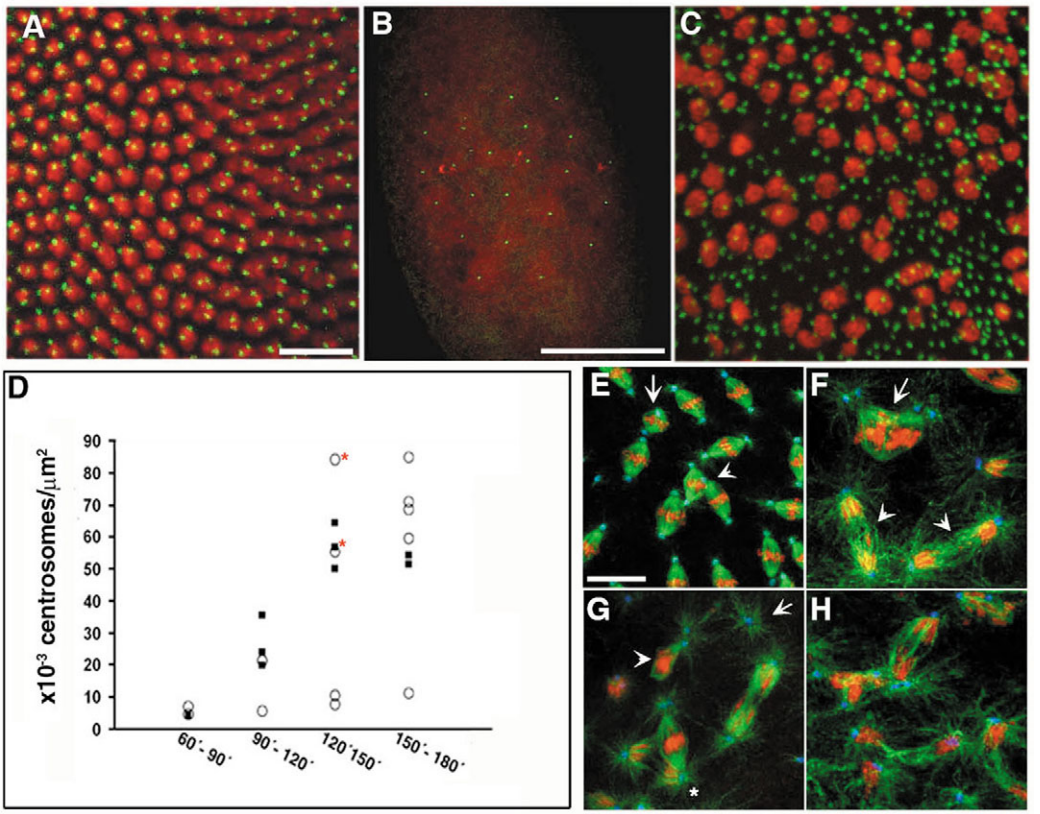

Fig. 4. Centrosome replication in *bubR1*^{Rev1} embryos. In all panels, DNA is in red, centrosomes are in (A-C) green or (E-H) blue with tubulin in green. (A) Cortical section of a 3 hour AEL wild-type embryo showing a homogeneous distribution of nuclei, each associated with a pair of centrosomes. (B) *bubR1*^{Rev1} embryo at 1 hour AEL showing well-separated centrosomes at the cortex and almost complete absence of nuclear DNA. (C) Cortical section of *bubR1*^{Rev1} embryo at 3 hours AEL showing regions with no nuclei and areas with large number of centrosomes. (D) Quantification of the number of centrosomes per area in either wild-type (black squares) or mutant embryos (white circles) at different times AEL (minutes). Asterisk refers to embryos in A,C. (E-H) Mitotic spindles at nuclear cycles 10-11 in *bubR1*^{Rev1} embryos. (E) Abnormal distribution of barrel-shaped spindles (arrow) showing centrosomes (arrowhead) abnormally close to a centrosome from an adjacent spindle. (F) Fused spindles without proper separation of centrosomes at the spindle poles (arrow); other spindles assemble normally but show lagging chromosomes during anaphase (arrowheads). (G) Monopolar spindles resulting from loss of centrosomes (arrowhead), spindles that share centrosomes (asterisk) and free centrosomes (arrow) are able to nucleate microtubules. (H) Excess centrosomes perturb spindle assembly and chromosomes segregation. Scale bars: 20 μm in A,C; 50 μm in B; 10 μm in E-H.

and centrosomes, suggesting that development had stopped completely.

Owing to the abnormal mitotic progression of *bubR1*^{Rev1} embryos, we looked at the ability of centrosomes to nucleate microtubules and to organise proper mitotic spindles. Although all the centrosomes we observed were able to nucleate microtubule asters, a detailed analysis showed several abnormalities in spindle organisation and distribution with strong variation within each embryo (Fig. 4E-H). Spindles were abnormally distributed within the syncytium and some spindles were shorter in length (Fig. 4E arrowhead and arrow). In other cases, we observed fused spindles while neighbouring nuclei display an almost normal anaphase onset with traces of chromosome bridges (Fig. 4F, arrow and arrowhead). Free centrosomes were observed to replicate asynchronously from the cycle of DNA replication and were able to nucleate microtubules (arrowhead and arrow in Fig. 4G,H). In addition, chromosomes from neighbouring nuclei often shared the same spindle pole (asterisk in Fig. 4K,H). These results indicate that the abnormal mitotic progression observed in *bubR1*^{Rev1} embryos uncoupled DNA and centrosomes cycle.

Mitotic progression in *bubR1*^{Rev1} embryos after spindle damage

Previous findings in somatic cells of many organisms showed that treatment with colchicine, a microtubule depolymerising agent, causes cells to arrest in a prometaphase-like state dependent upon BubR1 accumulation at kinetochores (Basu et al., 1999; Chan et al., 1998). However, although colchicine treatment of *Drosophila* embryos during syncytial stages causes a mitotic arrest (Zalokar and Erk, 1976), the role of spindle checkpoint proteins in this arrest has never been analyzed. Thus, 0-2 hours AEL, wild-type and *bubR1*^{Rev1} embryos were treated with colchicine at a concentration of 250 μM for 30 minutes and the mitotic arrest was monitored by immunodetection of Histone H3 phosphorylated at S10, which is diagnostic of mitotic chromosome condensation (Fig. 5). For quantitative analysis, we divided embryos into three categories, cycles 3 to 6, cycles 7 to 9 and cycles 10 to 13. The results show that after colchicine incubation, all nuclei in wild-type embryos arrest in a prometaphase-like state, with Phospho-Histone H3-positive chromatin (Fig. 5A,A′′,E) and strong accumulation of BubR1 at kinetochores (Fig. 5C). However, in *bubR1*^{Rev1} embryos, we observed a decrease in the proportion of nuclei showing mitotic arrest over time. Although 63% of the embryos at cycle 3-6 arrest, only 40% at cycle 7-9 and 23% at cycle 10-13 are Phospho-Histone H3 positive (Fig. 5E). The remaining embryos had mostly post-mitotic nuclei, Phospho-Histone H3 negative (Fig. 5B) with no BubR1 accumulation at kinetochores (Fig. 5D). Accordingly, our results demonstrate that BubR1 checkpoint activity is required during embryogenesis to allow mitotic arrest in response to spindle damage. In addition, our results suggest that BubR1 maternal supply from *bubR1*^{Rev1} allele although undetectable by western

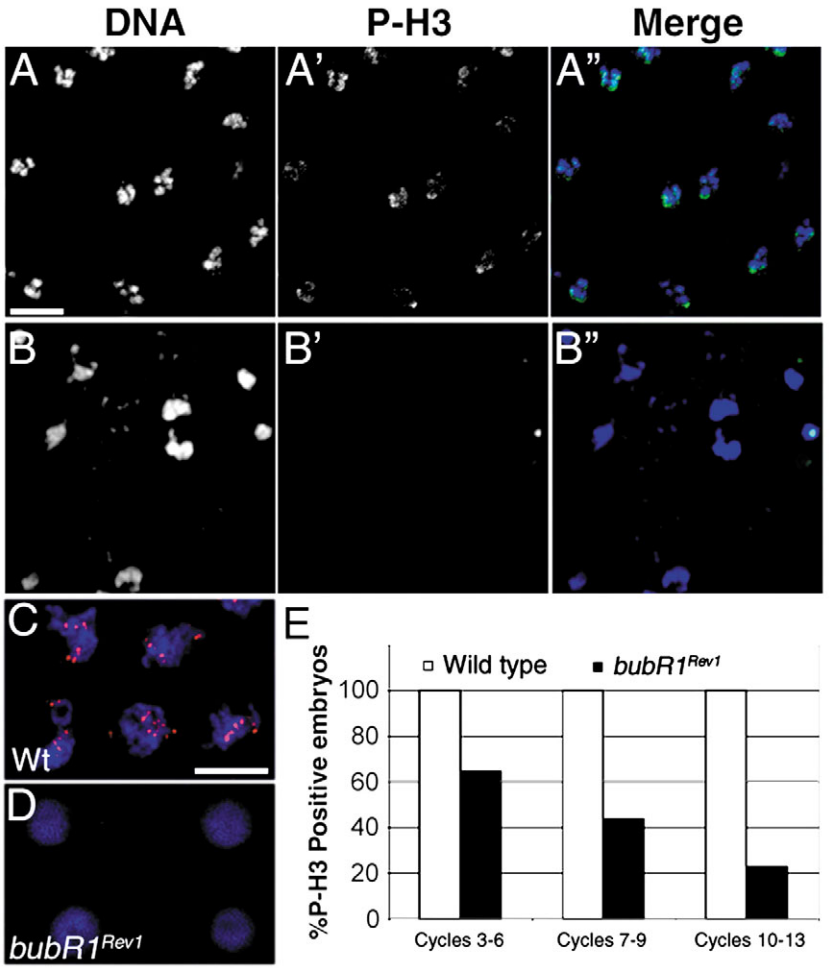

Fig. 5. Development of *bubR1*^{Rev1} embryos following spindle damage. Wild-type and *bubR1*^{Rev1} embryos at 0-3 hours AEL were incubated with colchicine during 30 minutes, fixed and immunostained with anti Phospho-Histone H3 antibodies. Merged images show DNA (blue), anti-PH3 (green) and BubR1 (red). Following colchicine treatment, (A,A′′) Wild-type nuclei arrest in a prometaphase-like stage and are Phospho-Histone H3 positive, while a significant proportion of *bubR1*^{Rev1} embryos are Phospho-Histone H3 negative (B,B′′). Following colchicine treatment, BubR1 accumulates at kinetochores of (C) wild-type prometaphase-like nuclei but is not detectable in (D) nuclei from *bubR1*^{Rev1} embryos. (E) Quantification of Phospho-Histone H3-positive embryos treated with colchicine during cycle 3-6, 7-9 and 10-13 (wild-type embryos: n=32 for cycle 3-6, n=21 for cycle 7-9 and n=37 for cycle 10-13. *bubR1*^{Rev1} embryos: n=54 for cycle 3-6, n=18 for cycle 7-9 and n=47 for cycle 10-13. We considered embryos positive when more than 80% of nuclei were Phospho-Histone H3 positive. Scale bar: 10 μm.

blotting of individual embryos is sufficient to support partial checkpoint activity during early nuclear cycles but as development proceeds it becomes limiting.

Polar body organisation in *bubR1^{Rev1}* embryos

The mature oocyte is arrested in metaphase of meiosis I and meiosis activation occurs during passage through the oviduct. Soon after activation, meiosis is resumed, even if fertilisation has not occurred. After meiosis II, the inner-most female pronucleus participates in zygotic development, while the three remaining haploid nuclei stay at the egg cortex and form the polar body after one round of replication and DNA condensation (Fig. 6A′′) (Foe et al., 1993). The polar body does not participate in further nuclear division cycles and maintains a mitotic-arrest configuration until cycle 8-10, when it falls into the interior of the embryo. In wild-type unfertilised (data not shown) and fertilised embryos, BubR1 accumulates strongly at the kinetochores of the polar body chromosomes where it co-localises with the centromere marker CID (Fig. 6A,A′′′). In order to assess whether organisation and/or maintenance of the mitotic arrest is dependent upon BubR1 localisation at polar body kinetochores, we analyzed its organisation in *bubR^{Rev1}* embryos. In unfertilised and fertilised embryos, we failed to detect any BubR1 accumulation at polar body kinetochores (Fig. 6B,C) and instead of a well-organised structure, we observed large masses of decondensed DNA with a spherical interphase-like conformation (Fig. 6B′′,C′′), presenting an increase number of CID-positive dots and suggesting that they undergo extra rounds of DNA replication (compare Fig. 6A′ with 6C′).

Subsequently, using Phospho-Histone H3 antibodies, we quantified the state of condensation of polar bodies in 0-90 minutes AEL wild-type and *bubR1^{Rev1}* embryos (Fig. 6H). In wild-type embryos either unfertilised (data not shown) or fertilised, polar bodies are always Phospho-Histone H3 positive (Fig. 6D′,H). However, in unfertilised *bubR1^{Rev1}*

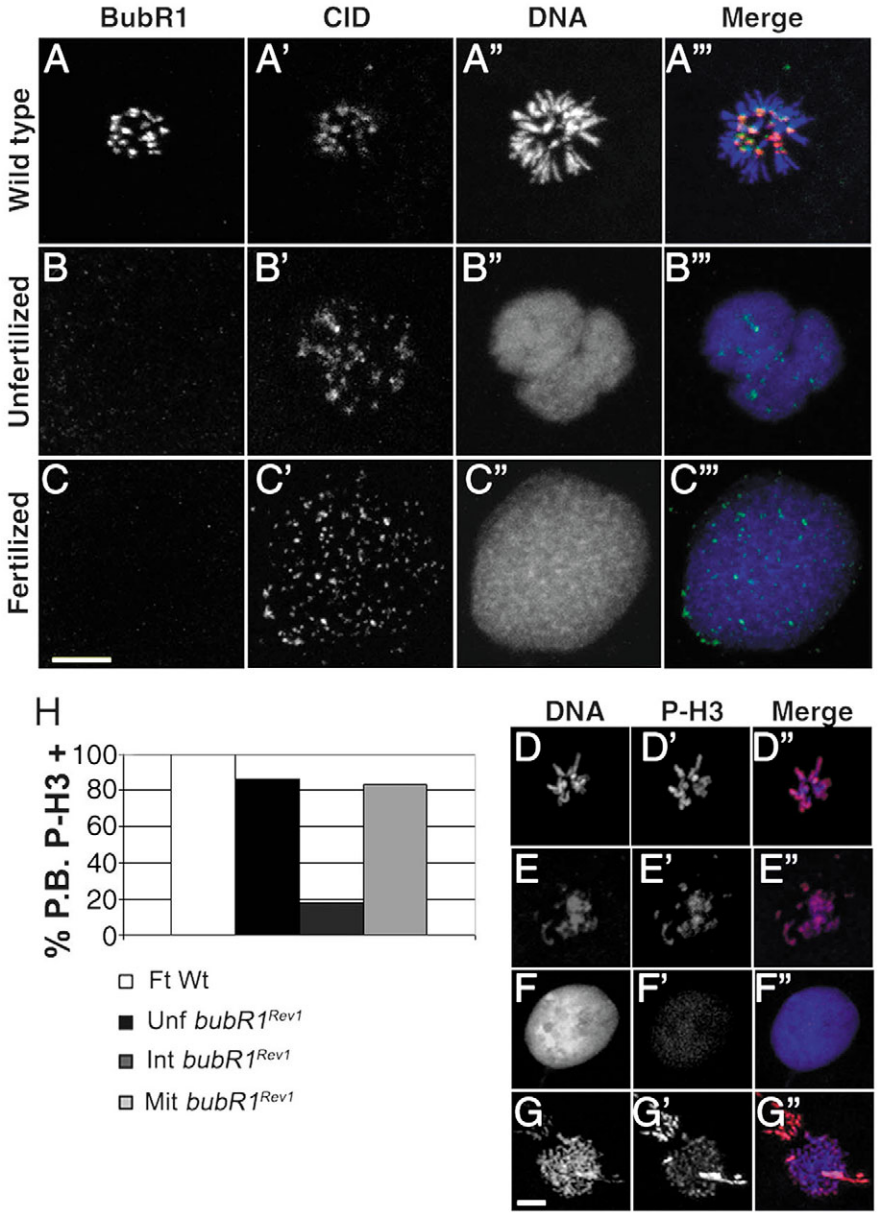

Fig. 6. Organisation of the polar body in wild-type and *bubR1^{Rev1}* embryos. (A-C) In merged images, BubR1 is in red, DNA in blue and CID in green. (A-A′′′) BubR1 localises at kinetochores of polar body chromosomes in wild-type embryos. (B,B′′′) In unfertilised *bubR1^{Rev1}* embryos, polar body chromosomes fail to maintain a prometaphase arrest and appear decondensed. (C,C′′′) In fertilised *bubR1^{Rev1}* embryos, polar body chromosomes are mostly decondensed and show an increased number of CID-positive signals. (D-G) DNA is in blue and Phospho-Histone H3 in red in merged images. (D,D′′) In wild-type embryos, polar bodies have condensed Phospho-Histone H3 positive chromosomes. (E,E′′) In unfertilised *bubR1^{Rev1}* embryos, polar bodies show DNA condensation with a low Phospho-Histone H3 signal and alteration of chromosome configuration. (F,F′′,G,G′′) In fertilised *bubR1^{Rev1}* embryos, the polar bodies follow cycles of condensation-decondensation. (F′) The polar body is Phospho-Histone H3 negative and shows a decondensed interphase-like state or (G-G′′) shows a low Phospho-Histone H3 positive labelling and partial DNA condensation. (H) Quantification of Phospho-Histone H3-positive polar bodies in wild-type and *bubR1^{Rev1}* embryos: fertilised wild-type embryos (Ft Wt, *n*=30), unfertilised *bubR1^{Rev1}* embryos (Unf *bubR1^{Rev1}*, *n*=30), fertilised *bubR1^{Rev1}* embryos with syncytial nuclei in interphase (Int *bubR1^{Rev1}*, *n*=11) and fertilised *bubR1^{Rev1}* embryos with syncytial nuclei in mitosis (Mit *bubR1^{Rev1}*, *n*=30). Scale bar: 10 μm.

embryos, we found that in 80% of the embryos (n=30) (Fig. 6H), polar bodies are Phospho-Histone H3 positive and their DNA appear condensed but without a normal chromosome organisation (compare Fig. 6D with 6E), whereas in fertilised embryos (n=41) the chromatin appeared to follow a cycle of condensation-decondensation, which seems to be in phase with the division cycles of the neighbouring nuclei (Fig. 6F,H). The cycle in polar body condensation-decondensation was not always complete and some Phospho-Histone H3 signal can be detected within the chromatin of decondensed polar body (Fig. 6G′).

Our observations of condensation-decondensation cycles, variation in Phospho-Histone H3 signal and increase number of CID-positive dots lead us to investigate whether in the absence of BubR1, the polar body became under the control of the mitotic oscillator that drives the nuclear cycles during the syncytial stages. Using a Histone-GFP transgene and time-lapse confocal microscopy, we recorded for a period of 40-80 minutes the polar body structure in wild type and *bubR1*^{Rev1} fertilised embryos collected at 0-30 min AEL (Fig. 7A,B, Movies 3 and 4 in the supplementary material). Then we quantified the relative Histone-GFP signal intensity over time (Fig. 7C) and calculated the pixel intensity±s.d. for the recorded period of time (Fig. 7D). As expected, in fertilised wild-type embryos the polar body always maintains a mitotic-arrest configuration during the recording period (Fig. 7A). The relative Histone-GFP signal over time remains constant with a low variation in pixel intensity (Fig. 7C,D). By contrast, *bubR1*^{Rev1} embryos display cycles of chromatin condensation and decondensation during the recorded period of time (Fig. 7B; Movie 4 in the supplementary material). Quantification of the relative Histone-GFP signal shows oscillation over time with a strong variation in pixel intensity for the recorded period of time, suggesting extra cycles of DNA replication (Fig. 7C,D). Indeed, although in wild type embryos, the polar body never incorporates BrdU, in *bubR1*^{Rev1} embryos, BrdU signal can be easily detected within the polar body chromosomes at 30-90 minutes AEL (Fig. 7D,E). Taken together, our results show that BubR1 is essential to maintain the mitotic arrest of the polar body and to prevent extra rounds of DNA replication.

Discussion

BubR1 is required during early embryonic development

Western blot analysis and immunodetection on stage 10 egg chambers revealed a maternal contribution for the highly conserved spindle checkpoint protein BubR1 to ensure normal progression through early stages of embryo development prior to the onset of zygotic gene expression. During syncytial

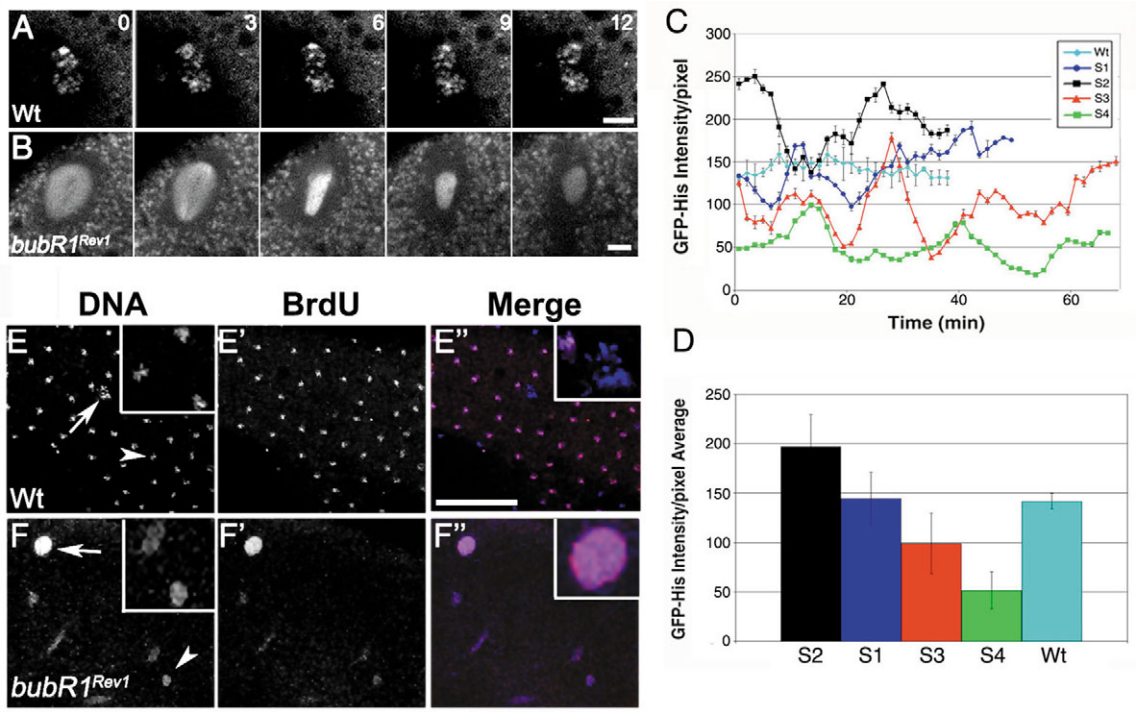

Fig. 7. Live imaging and BrdU incorporation of the polar body of wild-type and *bubR1*^{Rev1} embryos. (A,B) Time lapse imaging of polar bodies from fertilised (A) wild-type or (B) *bubR1*^{Rev1} embryos. In wild-type embryos, polar bodies do not change in structure and Histone-GFP signal level remains constant. In *bubR1*^{Rev1} embryos, polar bodies show cyclical changes in Histone-GFP signal intensity (see Movies 3 and 4 in the supplementary material). (C) Graphical representation of the relative Histone-GFP signal intensity/pixel in polar bodies of different embryos (wt, wild type; S1-4, *bubR1*^{Rev1} embryos). Oscillations in Histone-GFP signal intensity represent differences in DNA condensation and decondensation. (D) Graphical representation of the dynamic range of the raw data from C. (E,F) BrdU incorporation into fertilised (E,E′′) wild type or (F,F′′) *bubR1*^{Rev1} embryos. Arrows indicate polar bodies and arrowheads syncytial nuclei. BrdU incorporation occurs in the DNA of the *bubR1*^{Rev1} polar body and in all the nuclei in the interior of the embryo, but not in the polar body of wild-type embryos. In all merged images, DNA is stained blue and BrdU is stained red. Insets in merged images show higher magnifications of the polar body. Scale bars: 10 μm in A,B; 100 μm E,F.

divisions, BubR1 localisation correspond to previous description in *Drosophila* larval neuroblast and S2 cells (Basu et al., 1999), except for BubR1 localisation on spindle microtubules at metaphase. Dynein-dependent redistribution of BubR1 and other checkpoint proteins was previously observed in mammalian cells and *Drosophila* embryos (Basto et al., 2004; Howell et al., 2001; Wojcik et al., 2001). Accordingly, our observations of BubR1 localisation along spindle microtubules at metaphase suggests that during syncytial division, it could be partially removed from kinetochores via microtubule transport. As we only observe BubR1 spindle localisation in one third of the metaphases, we suspect that the removal and redistribution of BubR1 is likely to occur within a very short period of time at this stage. Further studies using live imaging in different mitotic cell populations in *Drosophila* will elucidate if our observation reflects different mechanism of BubR1 checkpoint regulation between the syncytial and somatic divisions.

In order to study BubR1 checkpoint activity during the syncytial nuclear divisions, we characterised *bubR1*^{Rev1}, a new hypomorphic female sterile allele. Analysis of nuclear proliferation in *bubR1*^{Rev1} embryos shows that starting at cycle 4-5 all embryos present abnormal mitotic progression as described for *bubR1*^{1} mutant allele (Basu et al., 1999). It has been previously shown that BubR1 is involved in chromosome alignment/congression (Ditchfield et al., 2003; Lampson and Kapoor, 2005) and in the inhibition of APC/C activity by signalling lack of tension at the kinetochore (Logarinho et al., 2004). The lagging chromatids, DNA bridges and aneuploidy observed in *bubR1*^{Rev1} embryos indicate precocious anaphase onset without stable microtubule-kinetochore attachment and an increase local degradation of APC/C targets. Therefore, our observations of mitotic progression on fix and live embryos, in addition to the failure to delay mitosis exit in the presence of colchicine, support the notion that BubR1 spindle checkpoint activity is required during the rapid nuclear proliferation of *Drosophila* embryo. In the absence of BubR1, nuclear mitotic exit is initiated too rapidly, resulting in nuclear cycle asynchrony and developmental failure.

BubR1 is essential to maintain the mitotic arrest of the polar body

In wild-type *Drosophila* embryo, three out of the four haploid meiotic products form the polar body which is formed by Phospho-H3-positive condensed chromosomes containing radiating microtubules without centrosomes (Foe et al., 1993). Although it has been hypothesised that F-actin and myosin II are involved into pulling and anchoring the polar body to the embryonic cortex with the plus ends of microtubules attached to the kinetochores and the minus ends facing outwards (Foe et al., 2000), the establishment and maintenance of the polar body mitotic arrest imply that specific factors are required to exclude it from the mitotic oscillation as it occurs in the same cytoplasm where neighbouring nuclei undergo synchronous divisions. Surprisingly, our immunodetection study revealed that BubR1 accumulates at polar body kinetochores in unfertilised and fertilised wild-type embryo. In *bubR1*^{Rev1} embryos; the polar body fail to establish and maintain its structure. Instead, polar bodies undergo cycle of DNA condensation-decondensation in phase with the mitotic cycle of the neighbouring nuclei. Thus, our results strongly suggest that at least the maintenance of the mitotic arrest and the exclusion of the polar body from the mitotic oscillator activity in the cytoplasm are dependent on normal BubR1 levels. Accordingly, BubR1 localisation at the polar body kinetochores appears to have a dominant effect by allowing maintenance of the arrest.

Similarly, it has been shown that the conserved mitotic checkpoint protein Mps1 is require for polar body mitotic arrest (Fischer et al., 2004) and while BubR1 polar body localisation is affected by Mps1 mutation, its nuclear syncytial localisation remains unaffected. Moreover, *gnu, png* and *plu* gene products which form a multi-protein complex have been shown to be required for entry and exit into mitosis during early syncytial cycles in *Drosophila* embryos through Cyclin B stabilisation (Fenger et al., 2000; Lee et al., 2003; Zhang et al., 2004). Mutant alleles of these genes induce nuclei to undergo DNA replication in the absence of chromosome segregation and polar body de-condensation. Furthermore, it has been shown that increase Cyclin B levels in a *png* mutant genetic background can restore polar body chromosome condensation (Lee et al., 2001). These observations lead us to speculate a potential genetic interaction between BubR1, Mps1 and *gnu-png-plu* during the syncytial stages. However, it remains to be determined whether Mps1 and BubR1 are involved in the same pathway during early syncytial cycles and polar body structure. Moreover, while polar body structure differs between *bubR1* and *gnu* mutant embryos, it is possible that they interact genetically to establish and maintain polar body structure through local cyclin B stabilisation.

BubR1 checkpoint activity is required for synchrony of nuclear divisions

It has been recently proposed that syncytial nuclear proliferation should be divided in three phases: a first phase of synchronous proliferation (cycle 1 to 6), a second phase being Cdk1/cyclinB dependent with local variation in metaphase-anaphase duration (cycle 7 to 10), and a third phase of meta-synchronous divisions that is DNA damage checkpoint dependent and shows an increase in the duration of interphase and M phases (Ji et al., 2004). Within each embryo, the total nuclear cycle time between cycles 7 until 10 remains equal, but those located at the centre undergo prolonged metaphase, which is compensated by a shorter anaphase/telophase. These variations are regulated by local Cdk1/cyclin B activity and the total cycle length can be modified and influenced by variation in cyclin B maternal gene dose (Ji et al., 2002; Ji et al., 2004; Stiffler et al., 1999). It has been proposed that the meta-synchronisation observed between cycle 7-10 is solely induced by cytoplasmic flux and local oscillation in Cdk1/cyclin B activity (Ji et al., 2004) and that early cycles are driven by the dynamics of the mitotic apparatus (Edgar et al., 1994). However, our observations that in *bubR1*^{Rev1} embryos almost half of the embryos show extensive loss of nuclear synchrony as early as cycle 4-5, suggests that BubR1 checkpoint activity could be directly involved in the process of nuclear synchrony.

As all nuclei share a common cytoplasm, a key factor in the regulation of mitotic progression is the transduction of a global state to the local nuclear level so as to ensure proper synchrony. Although the abnormal mitotic progression in *bubR1*^{Rev1} embryos can be easily explained in terms of spindle checkpoint activity, the nuclear cycle asynchrony suggests that BubR1

regulates the mitotic apparatus at a local level by timing the proper progression of chromosome congression and anaphase onset. It has been proposed that higher Cdk1/cyclin B activity decreases microtubule stability and increases sister chromatids velocity at anaphase to maintain constant nuclear cycle length within the embryo (Ji et al., 2004; Stiffler et al., 1999). Our observations suggest that local variation in BubR1 checkpoint activity can provide a feedback mechanism to ensure proper chromosome segregation and local variation in the timing of metaphase/anaphase transition through regulation of microtubule attachment/tension at kinetochore pairs and APC/C inhibition. However, our analysis of local cyclin B levels by immunodetection did not provide conclusive results, probably owing to the severe abnormalities we observed in *bubR1*^{Rev1} embryos (data not shown). Furthermore, as an increase in cyclin B copy number induces local changes in nuclear progression and only a global embryonic phenotype at six extra copies (Ji et al., 2002; Ji et al., 2004), our observations lead us to speculate that variation in BubR1/cyclin B copy number should induce local variation in timing mitotic progression without affecting the total embryonic phenotype. Accordingly, a decrease in BubR1 protein level should result in a decrease in metaphase delay during cycle 7, as well as a reduced metaphase delay induced by higher cyclin B levels.

In summary, our analysis of the requirement of BubR1 indicates that during syncytial development the spindle checkpoint appears to operate at various levels. It ensures that nuclei respond to global perturbations by imposing a mitotic arrest especially during later cycles. BubR1 also appears to work at a local level during early and late cycles to ensure proper synchrony of nuclear divisions. In parallel, BubR1 is required to sustain the mitotic arrest of the polar body so as to exclude it from undergoing further rounds of DNA replication during embryonic development.

We would like to thank G. Karpen and T. C. Kaufman for antibodies. We also thank Madalena Costa for help with colchicine treatment of embryos and all the members of the laboratory for comments and suggestions. D.P.-M. received a fellowship from l'ARC, France and N.M. was financed by a Training and Mobility grant from the European Union. The work in the laboratory of C. E. Sunkel is financed by grants from the Fundação para a Ciência e Tecnologia of Portugal and the European Union.

Supplementary material

Supplementary material for this article is available at
http://dev.biologists.org/cgi/content/full/132/20/4509/DC1

References

Basto, R., Scaerou, F., Mische, S., Wojcik, E., Lefebvre, C., Gomes, R., Hays, T. and Karess, R. (2004). In vivo dynamics of the rough deal checkpoint protein during Drosophila mitosis. *Curr. Biol.* **14**, 56-61.

Basu, J., Bousbaa, H., Logarinho, E., Li, Z., Williams, B. C., Lopes, C., Sunkel, C. E. and Goldberg, M. L. (1999). Mutations in the essential spindle checkpoint gene bub1 cause chromosome missegregation and fail to block apoptosis in Drosophila. *J. Cell Biol.* **146**, 13-28.

Blower, M. D. and Karpen, G. H. (2001). The role of Drosophila CID in kinetochore formation, cell-cycle progression and heterochromatin interactions. *Nat. Cell. Biol.* **3**, 730-739.

Callaini, G., Riparbelli, M. G. and Dallai, R. (1994). The distribution of cytoplasmic bacteria in the early Drosophila embryo is mediated by astral microtubules. *J. Cell Sci.* **107**, 673-682.

Chan, G. K., Schaar, B. T. and Yen, T. J. (1998). Characterization of the kinetochore binding domain of CENP-E reveals interactions with the kinetochore proteins CENP-F and hBUBR1. *J. Cell Biol.* **143**, 49-63.

Chen, R. H. (2002). BubR1 is essential for kinetochore localization of other spindle checkpoint proteins and its phosphorylation requires Mad1. *J. Cell Biol.* **158**, 487-496.

Clarkson, M. and Saint, R. (1999). A His2AvDGFP fusion gene complements a lethal His2AvD mutant allele and provides an in vivo marker for Drosophila chromosome behavior. *DNA Cell Biol.* **18**, 457-462.

Cooley, L., Kelley, R. and Spradling, A. (1988). Insertional mutagenesis of the Drosophila genome with single P elements. *Science* **239**, 1121-1128.

Debec, A., Kalpin, R. F., Daily, D. R., McCallum, P. D., Rothwell, W. F. and Sullivan, W. (1996). Live analysis of free centrosomes in normal and aphidicolin-treated Drosophila embryos. *J. Cell Biol.* **134**, 103-115.

Ditchfield, C., Johnson, V. L., Tighe, A., Ellston, R., Haworth, C., Johnson, T., Mortlock, A., Keen, N. and Taylor, S. S. (2003). Aurora B couples chromosome alignment with anaphase by targeting BubR1, Mad2, and Cenp-E to kinetochores. *J. Cell Biol.* **161**, 267-280.

Dobles, M., Liberal, V., Scott, M. L., Benezra, R. and Sorger, P. K. (2000). Chromosome missegregation and apoptosis in mice lacking the mitotic checkpoint protein Mad2. *Cell* **101**, 635-645.

Edgar, B. A., Sprenger, F., Duronio, R. J., Leopold, P. and O'Farrell, P. H. (1994). Distinct molecular mechanism regulate cell cycle timing at successive stages of Drosophila embryogenesis. *Genes Dev.* **8**, 440-452.

Fenger, D. D., Carminati, J. L., Burney-Sigman, D. L., Kashevsky, H., Dines, J. L., Elfring, L. K. and Orr-Weaver, T. L. (2000). PAN GU: a protein kinase that inhibits S phase and promotes mitosis in early Drosophila development. *Development* **127**, 4763-4774.

Fischer, M. G., Heeger, S., Hacker, U. and Lehner, C. F. (2004). The mitotic arrest in response to hypoxia and of polar bodies during early embryogenesis requires Drosophila Mps1. *Curr. Biol.* **14**, 2019-2024.

Foe, V. E., Odell, G. M. and Edgar, B. A. (1993). Mitosis and morphogenesis in the Drosophila embryo: point and counterpoint. In *The Development of Drosophila* (ed. M. Bate and A. M. Arias), pp. 149-300. New York: Cold Spring Harbor Laboratory Press.

Foe, V. E., Field, C. M. and Odell, G. M. (2000). Microtubules and mitotic cycle phase modulate spatiotemporal distributions of F-actin and myosin II in Drosophila syncytial blastoderm embryos. *Development* **127**, 1767-1787.

Fogarty, P., Campbell, S. D., Abu-Shumays, R., Phalle, B. S., Yu, K. R., Uy, G. L., Goldberg, M. L. and Sullivan, W. (1997). The Drosophila grapes gene is related to checkpoint gene chk1/rad27 and is required for late syncytial division fidelity. *Curr. Biol.* **7**, 418-426.

Heuer, J. G., Li, K. and Kaufman, T. C. (1995). The Drosophila homeotic target gene centrosomin (cnn) encodes a novel centrosomal protein with leucine zippers and maps to a genomic region required for midgut morphogenesis. *Development* **121**, 3861-3876.

Howell, B. J., McEwen, B. F., Canman, J. C., Hoffman, D. B., Farrar, E. M., Rieder, C. L. and Salmon, E. D. (2001). Cytoplasmic dynein/dynactin drives kinetochore protein transport to the spindle poles and has a role in mitotic spindle checkpoint inactivation. *J. Cell Biol.* **155**, 1159-1172.

Ji, J. Y., Haghnia, M., Trusty, C., Goldstein, L. S. and Schubiger, G. (2002). A genetic screen for suppressors and enhancers of the Drosophila cdk1-cyclin B identifies maternal factors that regulate microtubule and microfilament stability. *Genetics* **162**, 1179-1195.

Ji, J. Y., Squirrell, J. M. and Schubiger, G. (2004). Both cyclin B levels and DNA-replication checkpoint control the early embryonic mitoses in Drosophila. *Development* **131**, 401-411.

Kalitsis, P., Earle, E., Fowler, K. J. and Choo, K. H. (2000). Bub3 gene disruption in mice reveals essential mitotic spindle checkpoint function during early embryogenesis. *Genes Dev.* **14**, 2277-2282.

Lampson, M. A. and Kapoor, T. M. (2005). The human mitotic checkpoint protein BubR1 regulates chromosome-spindle attachments. *Nat. Cell. Biol.* **7**, 93-98.

Lee, L. A., Elfring, L. K., Bosco, G. and Orr-Weaver, T. L. (2001). A genetic screen for suppressors and enhancers of the Drosophila PAN GU cell cycle kinase identifies cyclin B as a target. *Genetics* **158**, 1545-1556.

Lee, L. A., Van Hoewyk, D. and Orr-Weaver, T. L. (2003). The Drosophila cell cycle kinase PAN GU forms an active complex with PLUTONIUM and GNU to regulate embryonic divisions. *Genes Dev.* **17**, 2979-2991.

Logarinho, E., Bousbaa, H., Dias, J. M., Lopes, C., Amorim, I., Antunes-Martins, A. and Sunkel, C. E. (2004). Different spindle checkpoint proteins monitor microtubule attachment and tension at kinetochores in Drosophila cells. *J. Cell Sci.* **117**, 1757-1771.

Musacchio, A. and Hardwick, K. G. (2002). The spindle checkpoint:

structural insights into dynamic signalling. *Nat. Rev. Mol. Cell. Biol.* **3**, 731-741.

O'Farrell, P. H., Stumpff, J. and Su, T. T. (2004). Embryonic cleavage cycles: how is a mouse like a fly? *Curr. Biol.* **14**, R35-R45.

Peters, J. M. (2002). The anaphase-promoting complex: proteolysis in mitosis and beyond. *Mol. Cell* **9**, 931-943.

Raff, J. W. and Glover, D. M. (1988). Nuclear and cytoplasmic mitotic cycles continue in Drosophila embryos in which DNA synthesis is inhibited with aphidicolin. *J. Cell Biol.* **107**, 2009-2019.

Roberts, D. B. (1986). Basic Drosophila care and techniques. In *Drosophila: A Practical Approach* (ed. D. B. Roberts), pp. 1-38. Oxford, England: IRL Press.

Sambrook, J., Fritsch, F. and Maniatis, T. (1989). *Molecular Cloning: A Laboratory Manual*, 2nd edn. Cold Spring Harbor, NY: Cold Spring Harbor Laboratory Press.

Sibon, O. C., Kelkar, A., Lemstra, W. and Theurkauf, W. E. (2000). DNA-replication/DNA-damage-dependent centrosome inactivation in Drosophila embryos. *Nat. Cell. Biol.* **2**, 90-95.

Stiffler, L. A., Ji, J. Y., Trautmann, S., Trusty, C. and Schubiger, G. (1999). Cyclin A and B functions in the early Drosophila embryo. *Development* **126**, 5505-5513.

Su, T. T., Sprenger, F., DiGregorio, P. J., Campbell, S. D. and O'Farrell, P. H. (1998). Exit from mitosis in Drosophila syncytial embryos requires proteolysis and cyclin degradation, and is associated with localized dephosphorylation. *Genes Dev.* **12**, 1495-1503.

Sullivan, W., Ashburner, M. and Hawley, R. S. (2000). *Drosophila Protocols*. Cold Spring Harbor: Cold Spring Harbor Laboratory Press.

Takada, S., Kelkar, A. and Theurkauf, W. E. (2003). Drosophila checkpoint kinase 2 couples centrosome function and spindle assembly to genomic integrity. *Cell* **113**, 87-99.

Wojcik, E., Basto, R., Serr, M., Scaerou, F., Karess, R. and Hays, T. (2001). Kinetochore dynein: its dynamics and role in the transport of the Rough deal checkpoint protein. *Nat. Cell. Biol.* **3**, 1001-1007.

Yu, K. R., Saint, R. B. and Sullivan, W. (2000). The Grapes checkpoint coordinates nuclear envelope breakdown and chromosome condensation. *Nat. Cell. Biol.* **2**, 609-615.

Zachariae, W. and Nasmyth, K. (1999). Whose end is destruction: cell division and the anaphase-promoting complex. *Genes Dev.* **13**, 2039-2058.

Zalokar, M. and Erk, I. (1976). Division and migration of nuclei during early embryogenesis. *J. Microbiol. Cell* **25**, 97-106.

Zhang, X. H., Axton, J. M., Drinjakovic, J., Lorenz, L., White-Cooper, H. and Renault, A. D. (2004). Spatial and temporal control of mitotic cyclins by the Gnu regulator of embryonic mitosis in Drosophila. *J. Cell Sci.* **117**, 3571-3578.